Multiphoton autoionization under strong laser radiation: Three-photon autoionization of strontium as a test case

Young Soon Kim
Department of Physics, University of Southern California, Los Angeles, California 90089

P. Lambropoulos
Department of Physics, University of Southern California, Los Angeles, California 90089
and Department of Physics, University of Crete, Iraklion, Crete, Greece
(Received 28 December 1983)

A theory of two- and three-photon autoionization is presented for intermediate resonant and nonresonant cases, stressing the laser-intensity effect on the configuration mixing of the final state. Sample calculations are performed for the $5p\,6s\ ^1P$ autoionizing state. The involvement of the $5s\,5d$ intermediate state includes the effects of ac Stark shifts on the ionization rate, the line shape, and the photoelectron angular distributions.

I. INTRODUCTION

The first observation[1] of multiply charged ions created by multiphoton ionization has by now been corroborated by a number of further experiments.[2–5] It has been established that alkaline earths and rare gases undergo even triple multiphoton ionization under laser intensities in the range of 10^{10}–10^{12} W/cm^2 and frequencies ranging from near infrared to ultraviolet. Although most reported observations dealt with either alkaline earths or rare gases, it appears that most atoms will behave similarly. In some of the more detailed experiments on alkaline earths,[2,3] it has been established that doubly excited and autoionizing states play perhaps the most significant role in this phenomenon which occurs at surprisingly low intensities, low in the context of multiphoton high-order processes. It has also been observed that such states undergo significant changes under the influence of the exciting radiation as evidenced by the substantial distortion of their line shape. Aside from the interest generated by these experiments from the standpoint of multiphoton spectroscopy, the high degree of excitation involved presents a challenging prospect for the creation of short-wavelength lasers.

There exists virtually no quantitative theoretical understanding of these processes. Going beyond the single-electron model of multiphoton ionization is the first step towards such understanding. For the alkaline earths this requires the inclusion of doubly excited states (above or below the first ionization threshold) in the description of the process. It further requires the inclusion of laser-intensity effects on such states beyond lowest-order perturbation theory. Given the observation of triply ionized species, it also raises the question of core excitation. In the case of rare gases, core excitation is of course the first question raised by multiple ionization.

Our purpose in this and following papers is to address these questions, beginning with an investigation of the participation of doubly excited states in the overall process. We formulate the problem in a way that permits the inclusion of intensity effects on the observable quantities. The specific system chosen for these calculations is atomic Sr because of the rather detailed experimental data available to us.

The results presented here aim at an assessment of the magnitude of observed and/or predicted effects. The work of Feldman, Welge, and collaborators[2,3] has provided the valuable stimulus and data for this analysis. More refined data will, however, be necessary if we are to arrive at quantitative comparison of theory with experiment.

Some of our initial results have been presented in an earlier paper.[6] Related calculations on H_2 have also been reported elsewhere.[7] A general discussion of this area of problems with more extended reference to related work can be found in some of our previous papers[8,9] on this subject.

II. MULTIPHOTON AUTOIONIZATION

A. Nonresonant two-photon autoionization

Autoionization can be formulated in terms of a transition from an initial bound state to a discrete state whose energy lies above the first ionization threshold and involves the excitation of at least two electrons. Usually, such an excited state couples to the continuum via configuration interaction and one must calculate the transition to both the discrete and the continuum parts. These two transitions interfere. In the usual treatment of autoionization, as given, for example, by Fano,[10] the discrete state is first coupled to the continuum by configuration interaction. The resulting new continuum states include the discrete, and the transition is then calculated through the appropriate transition matrix element between the initial bound state and the new prediagonalized continuum state.

For multiphoton autoionization, especially when the field is strong—in a sense to be specified below—this approach is insufficient. The field is no longer a weak probe that simply causes a transition proportional to its intensity. It is part of the interacting system, and since the coupling can be comparable to or even larger than the config-

uration interaction, the two must be treated on an equal footing. In that case, new behavior of the system is to be expected, while for a weak field, a generalization of the conventional equations to the multiphoton case should be obtained. Two new aspects should be incorporated, therefore, in the new formalism: The multiphoton aspect and the possibility that the field may become strong. Obviously, the latter can also occur when an autoionizing state is excited by a single-photon strong-field transition from a bound state. Formal aspects of this question have been discussed in recent papers.[8,11–13] Here we outline first the derivation of two-photon autoionization which then is easily generalized to the multiphoton case.

Let $|g\rangle$ be the initial (usually the ground) state, $|a\rangle$ the autoionizing state, and $|c\rangle$ the continuum to which $|a\rangle$ autoionizes. The two-photon transition from $|g\rangle$ to $|a\rangle$ and $|c\rangle$ occurs through a set of intermediate states $\{|b\rangle\}$ of the appropriate symmetry; which means that we have nonvanishing electric dipole matrix elements between $|g\rangle$ and $|b\rangle$, as well as between $|b\rangle$ and the states $|a\rangle$ and $|c\rangle$. They are here denoted by D_{bg}, D_{ab}, and D_{cb}, respectively, with D being the dipole operator written as

$$D=-e\vec{r}\cdot\vec{\epsilon}\mathscr{E}(t)\equiv\mu\mathscr{E}(t)\ , \tag{2.1}$$

where $\vec{\epsilon}$ is the polarization vector of the field and $\mathscr{E}(t)$ its amplitude. In terms of creation and annihilation operators, we have

$$\vec{\mathrm{E}}(t)\equiv\vec{\epsilon}\mathscr{E}(t)=i(2\pi\hbar\omega)^{1/2}[a(t)\vec{\epsilon}-a^{\dagger}(t)\vec{\epsilon}^{*}]\ , \tag{2.2}$$

where ω is the frequency of the field. Autoionization occurs through the interaction e^2/r_{12}, and the respective matrix element, including all the constants, is denoted by V_{ac}. The total Hamiltonian will be denoted by

$$H=H^A+H^R+D+V\ ,$$

where H^A and H^R are the Hamiltonians of the free atom (molecule) and radiation field, respectively. The states $|g\rangle$, $|a\rangle$, and $|c\rangle$ are to be understood as eigenstates of H^A. If $|n\rangle$ denotes the initial state of the radiation—which is assumed to contain n photons in a single mode of frequency ω—the states of interest for the uncoupled system "atom plus radiation" are the product states $|g\rangle|n\rangle$, $|b\rangle|n-1\rangle$, $|a\rangle|n-2\rangle$, and $|c\rangle|n-2\rangle$, for which we also use the abbreviated notation g', b', a', and c'. Their respective energies are

$$E_{g'}=E_g+n\hbar\omega,\quad E_{b'}=E_b+(n-1)\hbar\omega\ ,$$

$$E_{a'}=E_a+(n-2)\hbar\omega,\quad E_{c'}=E_c+(n-2)\hbar\omega\ ,$$

where E_g, E_b, E_a, and E_c are the energies of the bare atomic states. The states g', b', a', and c' are eigenstates of $H^0\equiv H^A+H^R$.

Now let $G(z)$ be the resolvent operator defined by

$$G(z)=\frac{1}{z-H}=\frac{1}{z-H^0-D-V} \tag{2.3}$$

in terms of which we obtain the time evolution operator $U(t)$ as the inverse Laplace transform of $G(z)$. At time $t=0$, the wave function of the system is $|g'\rangle$, while for $t>0$, it is obtained from $\Psi(t)=U(t)|g'\rangle$ which implies that only the matrix elements $U_{g'g'}$, $U_{b'g'}$, $U_{a'g'}$, and $U_{c'g'}$ are necessary for the prediction of the dynamical behavior of the system. Because of the initial condition, $U_{g'g'}(t=0)=1$, all others being zero for $t=0$. It follows then that we need only the corresponding matrix elements of G which, in an obvious abbreviated notation, we denote by $G_{g'}$, $G_{b'}$, $G_{a'}$, and $G_{c'}$. Writing Eq. (2.3) in the form $(z-H^0-D-V)G=1$, and taking the above matrix elements of both sides, we obtain

$$(z-E_{g'})G_{g'}-\sum_{b'}D_{g'b'}G_{b'}=1\ , \tag{2.4a}$$

$$-D_{b'g'}G_{g'}+(z-E_{b'})G_{b'}-D_{ba'}G_{a'}-\int dE_{c'}D_{b'c'}G_{c'}=0\ , \tag{2.4b}$$

$$-\sum_{b'}D_{a'b'}G_{b'}+(z-E_{a'})G_{a'}-\int dE_{c'}V_{a'c'}G_{c'}=0\ , \tag{2.4c}$$

$$-\sum_{b'}D_{c'b'}G_{b'}-V_{c'a'}G_{a'}+(z-E_{c'})G_{c'}=0\ . \tag{2.4d}$$

From these equations we derive the transition probability for autoionization, assuming first that none of the intermediate states b are in resonance with a single-photon transition from g. We assume, that is, a nonresonant two-photon transition from g to a and c. Eliminating $G_{b'}$, by solving Eq. (2.4b) for $G_{b'}$ and substituting into the other equations, we obtain

$$(z-E_{g'})G_{g'}-\sum_{b'}\frac{D_{g'b'}D_{b'a'}}{E_{g'}-E_{b'}}G_{a'}-\sum_{b'}\int dE_{c'}\frac{D_{g'b'}D_{b'c'}}{E_{g'}-E_{b'}}G_{c'}=1\ , \tag{2.5a}$$

$$-\sum_{b'}\frac{D_{a'b'}D_{b'g'}}{E_{g'}-E_{b'}}G_{g'}+(z-E_{a'})G_{a'}-\int dE_{c'}\left[V_{a'c'}+\sum_{b'}\frac{D_{a'b'}D_{b'c'}}{E_{g'}-E_{b'}}\right]G_{c'}=0\ , \tag{2.5b}$$

$$-\sum_{b'}\frac{D_{c'b'}D_{b'g'}}{E_{g'}-E_{b'}}G_{g'}-\left[V_{c'a'}+\sum_{b'}\frac{D_{c'b'}D_{b'a'}}{E_{g'}-E_{b'}}\right]G_{a'}+(z-E_{c'})G_{c'}=0\ , \tag{2.5c}$$

which are valid on the condition that the energy differences $E_b-E_g-\hbar\omega$ for all b be much larger than the width (spontaneous as well as induced) of state $|b\rangle$. On the basis of this condition, we have also neglected terms that involve $|D_{g'b'}|^2$ and $|D_{a'b'}|^2$ which represent Rabi frequencies (induced lifetimes of $|b\rangle$) and $|D_{c'b'}|^2$ which represents the ionization width of $|b\rangle$. Nonresonant two-photon ionization (or equivalently, large detuning) implies that such quantities are small compared to $E_g-E_b+\hbar\omega$. When this condition is satisfied, the energy differences $E_a-E_b-\hbar\omega$ are also large since we assume $2\hbar\omega\cong E_a-E_g$, i.e., we examine the behavior around an isolated autoionizing resonance. It is the same condition that also enables us to replace z by $E_{g'}$ in the denominators $z-E_{b'}$ which result from solving Eq. (2.4b) for $G_{b'}$.

We introduce now the following effective two-photon

matrix elements:

$$D^{(2)}_{a'g'}=\sum_{b'}\frac{D_{a'b'}D_{b'g'}}{E_{g'}-E_{b'}}=\mathscr{E}^2\sum_b\frac{\mu_{ab}\mu_{bg}}{E_g-E_b+\hbar\omega}\equiv\mathscr{E}^2\mu^{(2)}_{ag}\ , \tag{2.6a}$$

$$D^{(2)}_{c'g'}=\sum_{b'}\frac{D_{c'b'}D_{b'g'}}{E_{g'}-E_{b'}}=\mathscr{E}^2\sum_b\frac{\mu_{cb}\mu_{bg}}{E_g-E_b+\hbar\omega}\equiv\mathscr{E}^2\mu^{(2)}_{cg}\ , \tag{2.6b}$$

$$D^{(2)}_{c'a'}=\sum_{b'}\frac{D_{c'b'}D_{b'a'}}{E_{g'}-E_{b'}}=\mathscr{E}^2\sum_b\frac{\mu_{cb}\mu_{ba}}{E_g-E_b+\hbar\omega}\equiv\mathscr{E}^2\mu^{(2)}_{ca}\ , \tag{2.6c}$$

where, as usual, summation over b implies integration over the continuous part of the spectrum. An additional effective matrix element of a different type is suggested by Eq. (2.5) and is defined by

$$\tilde{V}_{c'a'}\equiv V_{c'a'}+D^{(2)}_{c'a'}=V_{ca}+\mathscr{E}^2\mu^{(2)}_{ca}\ . \tag{2.7}$$

Since V does not operate on radiation states, we have $V_{c'a'}=V_{ca}$. It must be kept in mind that V_{ca} is independent of the laser, while $D^{(2)}_{c'a'}$ is proportional to the laser intensity I.

In terms of the above effective matrix elements, Eqs. (2.5) now read

$$(z-E_{g'})G_{g'}-D^{(2)}_{g'a'}G_{a'}-\int dE_{c'}D^{(2)}_{g'c'}G_{c'}=1\ , \tag{2.8a}$$

$$-D^{(2)}_{a'g'}G_{g'}+(z-E_{a'})G_{a'}-\int dE_{c'}\tilde{V}_{a'c'}G_{c'}=0\ , \tag{2.8b}$$

$$-D^{(2)}_{c'g'}G_{g'}-\tilde{V}_{c'a'}G_{a'}+(z-E_{c'})G_{c'}=0\ . \tag{2.8c}$$

In form, these equations seem identical to those that couple an initial state $|g\rangle$ to an autoionizing state $|a\rangle$ and a continuum $|c\rangle$ via a single-photon transition, as can be readily verified by comparing with Eq. (4.8) of Ref. 11. In the present case, however, the coupling matrix elements, instead of being simple matrix elements of D and V, are effective matrix elements of second order in D and therefore dependent on laser intensity. As we will see below, this introduces significantly new behavior.

The continuum can be eliminated now by solving (2.8c) for $G_{c'}$ and substituting into the other equations, thus obtaining

$$\left[z-E_{g'}-\int dE_{c'}\frac{|D^{(2)}_{c'g'}|^2}{z-E_{c'}}\right]G_{g'}-\left[D^{(2)}_{g'a'}+\int dE_{c'}\frac{D^{(2)}_{g'c'}\tilde{V}_{c'a'}}{z-E_{c'}}\right]G_{a'}=1\ , \tag{2.9a}$$

$$-\left[D^{(2)}_{a'g'}+\int dE_{c'}\frac{\tilde{V}_{a'c'}D^{(2)}_{c'g'}}{z-E_{c'}}\right]G_{g'}+\left[z-E_{a'}-\int dE_{c'}\frac{|\tilde{V}_{c'a'}|^2}{z-E_{c'}}\right]G_{a'}=0\ . \tag{2.9b}$$

By analogy with the single-photon case, we can proceed as in Sec. IV of Ref. 11. We replace z by $E_{g'}+i\eta$ in the denominators above and then take the limit for $\eta\to+0$. The integrals over E_c separate then into a real and an imaginary part according to the identity

$$\lim_{\eta\to+0}\frac{1}{y+i\eta}=\mathrm{P}\frac{1}{y}-i\pi\delta(y)\ , \tag{2.10}$$

where P denotes the principal value. Letting $z\to E_{g'}+i\eta$ in the denominators, we note that $E_{g'}-E_{c'}=E_g+2\hbar\omega-E_c$ and that $E_g+2\hbar\omega$ is the energy above the initial state to which the two absorbed photons raise the system. It is the excitation energy and will be denoted by E. Since we are dealing with transitions above at least the first ionization threshold, E is a continuous variable as is ω and all quantities of interest for the description of the phenomenon will, in general, be functions of E. In particular, it is the transition probability that we wish to describe as a function of E. Another useful parameter is the detuning from resonance with the state $|a\rangle$ defined by

$$\delta=E-E_a=E_g+2\hbar\omega-E_a=2\hbar\omega-(E_a-E_g)\ . \tag{2.11}$$

Using the above definitions, we have

$$\int dE_{c'}\frac{|D^{(2)}_{c'g'}|^2}{z-E_{c'}}\to\mathrm{P}\int dE_c\frac{I^2|\mu^{(2)}_{cg}|^2}{E-E_c}-i\pi|\mu^{(2)}_{cg}|^2_{E_c=E}I^2$$

$$\equiv S_g-\frac{i}{2}\gamma_g\ , \tag{2.12a}$$

$$\int dE_{c'}\frac{|\tilde{V}_{c'a'}|^2}{z-E_{c'}}\to\mathrm{P}\int dE_c\frac{|\tilde{V}_{ca}|^2}{E-E_c}-i\pi|\tilde{V}_{ca}|_{E_c=E}$$

$$\equiv F_a-\frac{i}{2}\Gamma_a\ , \tag{2.12b}$$

and

$$D^{(2)}_{a'g'}+\int dE_{c'}\frac{\tilde{V}_{a'c'}D^{(2)}_{c'g'}}{z-E_{c'}}$$

$$\to\mathscr{E}^2\mu^{(2)}_{ag}+\mathrm{P}\int dE_c\frac{\tilde{V}_{ac}\mu^{(2)}_{cg}\mathscr{E}^2}{E-E_c}-i\pi(\tilde{V}_{ac}\mu^{(2)}_{cg})_{E_c=E}\mathscr{E}^2$$

$$\equiv\tilde{D}^{(2)}_{Eg}(1-i/\tilde{q})\ , \tag{2.12c}$$

where $I\equiv|\mathscr{E}|^2$ is the light intensity. The quantities S_g and γ_g are, respectively, the ac Stark shift and the ionization width of state $|g\rangle$ due to its direct (two-photon) coupling to the continuum, very much like in single-photon autoionization [see, for example, Eqs. (4.15)–(4.17) of Ref. 11]. In the present case, however, these quantities are not linear in the light intensity but quadratic because they represent two-photon processes. The quantities F_a and Γ_a are, respectively, the shift and width of $|a\rangle$ due to its coupling to the continuum through $\tilde{V}_{ac}$. In usual weak-field autoionization, $\tilde{V}_{ac}$ reduces to V_{ac} which makes F_a and Γ_a field-independent parameters of the bare atom. For arbitrary intensity, they again represent the shift and width of $|a\rangle$ due to configuration interaction V modified by the field through the presence of the term $\mathscr{E}^2\mu^{(2)}_{ac}$ representing a two-photon matrix element coupling $|a\rangle$ to $|c\rangle$. It corresponds to stimulated emis-

sion and subsequent absorption of a photon from $|a\rangle$ to $|c\rangle$ or vice versa as depicted pictorially in Fig. 1. It modifies, therefore, the effect of V_{ac} and the resulting width Γ_a can no longer be viewed as the conventional autoionization width because now it depends on the field intensity. We shall retain the term autoionization width, nevertheless, in order to distinguish it from the direct ionization width γ_g. Although these two quantities refer to different states, $|a\rangle$ and $|g\rangle$, respectively, they both represent ionization of the atom (transition into the continuum). All of the above shifts and widths, in principle, are functions of the total excitation energy E. For the moment we shall suppress this dependence, assuming it to be very weak, and the above quantities shall be treated as constants taking their value at E_a, or at $E_a+F_a(E_a)$ if F_a is significant. This assumption is not necessary and can easily be dropped in an actual calculation.

A note on the difference between S_g and F_a is perhaps useful at this point. The shift F_a at $\mathscr{E}=0$ is model dependent in the sense that its value is affected very much by how good the zeroth-order Hamiltonian and hence its wave functions are in representing the energy of the autoionizing resonance. In that sense it can be viewed as an artifact of the calculation. The energy of the physical state is E_a+F_a. On the other hand, the shift S_g (or any other ac Stark shift) is a real effect. It is unavoidably caused by the same radiation that causes the transition and is independent on the atomic model. Of course for $\mathscr{E}\neq 0$, F_a also contains a field-dependent contribution. Two additional quantities have been introduced in writing Eq. (2.12c). They are

$$\tilde{D}_{Eg}^{(2)} \equiv \mathscr{E}^2\mu_{ag}^{(2)} + \mathrm{P}\int dE_c \frac{\tilde{V}_{ac}\mu_{cg}^{(2)}}{E-E_c} \tag{2.13a}$$

and

$$\tilde{q} \equiv \frac{\tilde{D}_{Eg}^{(2)}}{\pi(\tilde{V}_{ac}\mu_{cg}^{(2)})_{E_c=E}} = \frac{\mu_{ag}^{(2)} + \mathrm{P}\int dE_c[\tilde{V}_{ac}\mu_{cg}^{(2)}/(E-E_c)]}{\pi[(V_{ac}+\mathscr{E}^2\mu_{ac}^{(2)})\mu_{cg}^{(2)}]_{E_c=E}} . \tag{2.13b}$$

As in conventional single-photon autoionization, $\tilde{D}_{Eg}^{(2)}$ represents a transition amplitude from the initial state to the autoionizing state modified by an admixture of the continuum. In the limit of zero coupling to the continuum ($\tilde{V}_{ac}\to 0$), it simply represents the Rabi frequency between $|g\rangle$ and $|a\rangle$. Here, however, it is a two-photon (second-order) matrix element, because it takes two photons of the assumed frequency to reach a state above threshold. In addition, it contains a new feature. It is not simply proportional to some power of the field, but it involves a more complicated nonlinear dependence through the presence of $\tilde{V}_{ac}$. Similarly, the parameter $\tilde{q}$ appears playing the same formal role as the usual q parameter of autoionization, except that now it depends on the radiation intensity in a nonlinear fashion through V_{ac}. Thus it no longer represents an atomic (molecular) parameter, but one that reflects the interaction with the field as well.

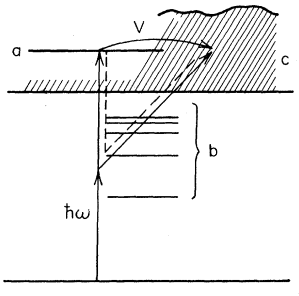

FIG. 1. Schematic diagram for two-photon autoionization.

Exploiting further the formal similarity with conventional autoionization, we can write the transition probability per unit time as

$$W = 2\pi |D_{cg}^{(2)}|^2 \frac{(\epsilon+\tilde{q})^2}{\epsilon^2+1} = 2\pi I^2 |\mu_{cg}^{(2)}|^2 \frac{(\epsilon+\tilde{q})^2}{\epsilon^2+1} \tag{2.14}$$

where ϵ is the detuning from the autoionizing state given by

$$\epsilon = \frac{E-E_a-F_a}{\frac{1}{2}\Gamma_a} = \frac{2\hbar\omega-(E_a+F_a-E_g)}{\frac{1}{2}\Gamma_a} . \tag{2.15}$$

As long as the intensity is sufficiently low for $\mathscr{E}^2\mu_{ac}^{(2)}$ in Eq. (2.7) to be negligible compared to V_{ac}, all of the above equations are identical to those of single-photon, weak-field autoionization and have the same physical content, except that all matrix elements involving the interaction with the radiation are of second order. In that case $\tilde{q}$ and Γ_a are the usual parameters, and the transition probability and line shape are features of the atom (molecule). For higher intensities, $\mathscr{E}^2\mu_{ac}^{(2)}$ becomes comparable to V_{ac}, the transition probability and line shape will change as functions of intensity in a nontrivial fashion. Equation (2.14) is still vaild, but different $\tilde{q}$, Γ_a, and line shapes will result for different intensities. Such changes can be qualitatively significant. Note, for example, that if the sign of $\mathscr{E}^2\mu_{ac}^{(2)}$ happens to be opposite to that of V_{ac}, the quantities $\tilde{V}_{ac}$ and Γ_a may, in principle, vanish at the appropriate intensity, while at the same time $\tilde{q}\to\infty$. Whether Γ_a can actually be observed to vanish in an experiment is, of course, doubtful because the competition with other channels as well as the finite laser bandwidth will tend to smooth out such drastic changes of Γ_a. The salient point, nevertheless, is that qualitative changes are apt to appear in line shapes and transition probabilities at intensities such that $I|\mu_{ac}^{(2)}| \cong |V_{ac}|$.

B. Resonant two-photon autoionization

The previous derivation is valid as long as the photon frequency ω is far from resonance with any intermediate state $|b\rangle$. If, on the other hand, for some b we have $E_b-E_g\cong\hbar\omega$, then some of the previous approximations are not valid. The most rigorous way of handling that case is to return to Eq. (2.4) and retain only one (the near-resonant) state $|b\rangle$, thus reducing the problem to one with three discrete states and one continuum. The continuum can then be eliminated as before by eliminating $G_{c'}$, which leads to a system of three equations for

$G_{g'}$, $G_{b'}$, and $G_{a'}$. These equations have been derived in Ref. 11 following exactly this procedure [see Eq. (5.17) of Ref. 11]. In the notation of Sec. II A with the primes dropped and $z-E_g$ replaced by z, they can be written as

$$zG_g-\Omega_1 G_b=1\ , \tag{2.16a}$$

$$-\Omega_1 G_g+\left[z+\delta_1+\frac{i}{2}\gamma_b\right]G_b-\tilde{\Omega}_2^*\left[1-\frac{i}{q}\right]G_a=0\ , \tag{2.16b}$$

$$-\tilde{\Omega}_2\left[1-\frac{i}{q}\right]G_b+\left[z+\delta+\frac{i}{2}\Gamma_a\right]G_a=0\ , \tag{2.16c}$$

where $\delta_1\equiv\hbar\omega-\bar{E}_{bg}$, $\delta\equiv 2\hbar\omega-\bar{E}_{ag}$, $\Omega_1\equiv\mathscr{E}\mu_{bg}$,

$$\tilde{\Omega}_2\equiv\mathscr{E}\left[\mu_{ab}+\mathrm{P}\int dE_c\frac{V_{ac}\mu_{cb}}{E-E_c}\right],\quad \tfrac{1}{2}\Gamma_a=\pi\,|\,V_{ca}\,|^2_{E_c=E}\ ,$$

and

$$\tfrac{1}{2}\gamma_b=\tfrac{1}{2}\gamma_b^0+\pi I\,|\,\mu_{cb}\,|^2_{E_c=E}\ .$$

The energy differences $\bar{E}_{bg}$ and $\bar{E}_{ag}$ are the differences of the respective atomic energies including the associated ac Stark shifts as well as the shift F_a of E_a. The expression for the width γ_b of the resonant intermediate state given above differs slightly from that of Ref. 11 in that it contains the additional contribution γ_b^0 due to the spontaneous decay of $|\,b\,\rangle$. This contribution may be of some significance for low intensities in the applications of this paper. Finally, Ω_1 is the Rabi frequency for the transition $|\,g\,\rangle\leftrightarrow|\,b\,\rangle$, while $\tilde{\Omega}_2$ is a generalized Rabi frequency for the transition $|\,b\,\rangle\leftrightarrow|\,a\,\rangle$. It is generalized in that it contains the effect of the admixture of the continuum through V_{ca}. The q parameter appearing in these equations is the usual q defined for autoionization from $|\,b\,\rangle$ and is therefore given by $q=\tilde{\Omega}_2/\pi V_{ac}D_{cb}$.

The general solution is obtained by solving Eqs. (2.16) exactly, which involves finding the roots of the third-order algebraic equation resulting from the determinant of the coefficients. The inverse Laplace transforms of G_g, G_b, and G_a are then expressed as linear combinations of three exponentials involving the three roots z_1, z_2, and z_3. The total ionization is then expressed as a function of time in the form $P_{\mathrm{ion}}(t)=1-|\,U_{gg}(t)\,|^2-|\,U_{bg}(t)\,|^2$. Although formal analytical solutions can be written in terms of the algebraic expressions for z_1, z_2, and z_3, they are of little value because of their complexity. Thus any useful information about ionization must be obtained numerically. Part of this has been done in Ref. 11. For large field intensities, ionization will be a function of time not expressible in terms of a time-independent transition probability per unit time. For relatively low intensities, on the other hand, that satisfy the inequality $\Omega_1\ll\gamma_b,\Gamma_a,|\,\tilde{\Omega}_2\,|$, the transition probability per unit time can be put in the (time-independent) form

$$\frac{dP}{dt}=\gamma_b\Omega_1^2\frac{\Gamma_a^2(\epsilon+q)^2}{4\,|\,f(\delta_1)\,|^2}\ , \tag{2.17a}$$

where

$$f(\delta_1)\equiv\left[\delta_1+\frac{i}{2}\gamma_b\right]\left[\delta+\frac{i}{2}\Gamma_a\right]-\tilde{\Omega}_2^2\left[1-\frac{i}{q}\right]^2\ . \tag{2.17b}$$

Although formally this equation allows for a detuning δ_1, from the intermediate state $|\,b\,\rangle$, it is understood that δ_1 should not be so large as to make the presence of other intermediate states significant thus invalidating the approximation of a single intermediate state. It is worth noting in passing that this equation is also applicable to the case of strong coupling between $|\,b\,\rangle$ and $|\,a\,\rangle$ as long as Ω_1 is weak, i.e., satisfies the above inequality. Experimentally, this can be achieved by using two lasers so as to control independently the strengths of the couplings $|\,g\,\rangle\leftrightarrow|\,b\,\rangle$ and $|\,b\,\rangle\leftrightarrow|\,a\,\rangle$.

C. Three-photon autoionization

The generalization to the three-photon case is straightforward. We do, however, present here a brief summary of the main equations in order to underscore certain nontrivial differences with the previous case and also to establish the formal framework for the specific calculations that follow.

Since it takes three photons to cross the ionization threshold, we have a double summation over intermediate states. If the first or the second photon leads to a resonant transition to a particular intermediate state, one of the sums collapses to a single term. In that case, the resonant formalism must be used, as we elaborate below. We shall be particularly interested in the case of two-photon resonant three-photon autoionization.

To set up the equation for the nonresonant case, we consider the initial state $|\,g\,\rangle$, a set of intermediate states $\{|\,b\,\rangle\}$ connected to $|\,g\,\rangle$ by a dipole transition and a second set of intermediate states $\{|\,d\,\rangle\}$ connected to $|\,b\,\rangle$, to the autoionizing state $|\,a\,\rangle$, and to the continuum $|\,c\,\rangle$ by a dipole transition. In general, $|\,g\,\rangle$ will be connected to $|\,a\,\rangle$ and $|\,c\,\rangle$ by an effective three-photon matrix element which is obtained through the elimination of the intermediate states. We would begin with the equations for the matrix elements of G which are the equivalent of Eqs. (2.4). We would then eliminate G_b and G_d, thus obtaining the effective three-photon matrix elements. Without showing here any of the tedious manipulations, we proceed to quote the resulting equations under the assumption that neither single nor two-photon resonances appear. The equations are

$$\left[z-E_{g'}-\int dE_{c'}\frac{|\,D^{(3)}_{c'g'}\,|^2}{z-E_{c'}}\right]G_{g'}-\left[D^{(3)}_{g'a'}+\int dE_{c'}\frac{D^{(3)}_{g'c'}\tilde{V}_{c'a'}}{z-E_{c'}}\right]G_{a'}=1\ , \tag{2.18a}$$

$$-\left[D^{(3)}_{a'g'}+\int dE_{c'}\frac{\tilde{V}_{a'c'}D^{(3)}_{c'g'}}{z-E_{c'}}\right]G_{g'}+\left[z-E_{a'}-\int dE_{c'}\frac{|\,\tilde{V}_{c'a'}\,|^2}{z-E_{c'}}\right]G'_a=0\ , \tag{2.18b}$$

where $|\,g'\,\rangle=|\,g\,\rangle|\,n\,\rangle$, $|\,a'\,\rangle=|\,a\,\rangle|\,n-3\,\rangle$, $|\,c'\,\rangle$

$=|c\rangle|n-3\rangle$, and $E_{g'}=E_g+n\hbar\omega$, $E_{a'}=E_a+(n-3)\hbar\omega$, $E_{c'}=E_c+(n-3)\hbar\omega$. The total excitation energy is $E=E_{g'}$, as in the two-photon case. The continuum has also been eliminated in the above equations. By making the substitution $z\rightarrow E_{g'}+i\eta$ and proceeding as in the previous case, we obtain the corresponding shifts, widths, etc., given by the following expressions:

$$S_g=\mathrm{P}\int dE_c\frac{I^3|\mu_{cg}^{(3)}|^2}{E-E_c}+\sum_b\frac{|\mu_{bg}|^2}{E_g-E_b+\hbar\omega}|\mathscr{E}|^2, \tag{2.19a}$$

$$\tfrac{1}{2}\gamma_g=\pi|\mu_{cg}^{(3)}|_{E_c=E}I^3,$$

$$F_a=\mathrm{P}\int dE_c\frac{|\tilde{V}_{ca}|^2}{E-E_c},\quad \tfrac{1}{2}\Gamma_a=\pi|\tilde{V}_{ca}|^2_{E_c=E}, \tag{2.19b}$$

$$D_{a'g'}^{(3)}+\int dE_{c'}\frac{\tilde{V}_{a'c'}D_{c'g'}^{(3)}}{E+i\eta-E_{c'}}$$
$$=\mathscr{E}^3\mu_{ag}^{(3)}+\mathrm{P}\int dE_c\frac{\tilde{V}_{ac}\mu_{cg}^{(3)}\mathscr{E}^3}{E-E_c}-i\pi(\tilde{V}_{ac}\mu_{cg}^{(3)})_{E_c=E}\mathscr{E}^3$$
$$\equiv\tilde{D}_{Eg}^{(3)}(1-i/\tilde{q}), \tag{2.19c}$$

where the three-photon effective matrix elements appearing above are defined by

$$\mu_{cg}^{(3)}=\sum_d\sum_b\frac{\langle c|\mu|d\rangle\langle d|\mu|b\rangle\langle b|\mu|g\rangle}{(E_d-E_g-2\hbar\omega)(E_b-E_g-\hbar\omega)}, \tag{2.20a}$$

$$\mu_{ag}^{(3)}=\sum_d\sum_b\frac{\langle a|\mu|d\rangle\langle d|\mu|b\rangle\langle b|\mu|g\rangle}{(E_d-E_g-2\hbar\omega)(E_b-E_g-\hbar\omega)}. \tag{2.20b}$$

The modified V, however, is still given by the expression

$$\tilde{V}_{ca}=V_{ca}+\mathscr{E}^2\mu_{ca}^{(2)}=V_{ca}+\mathscr{E}^2\sum_d\frac{\mu_{cd}\mu_{da}}{E_g-E_d+2\hbar\omega} \tag{2.21}$$

because we are interested in retaining only the lowest-order correction to V_{ca} which is of second order in $\mathscr{E}$ even though the lowest-order coupling between $|g\rangle$ and $|a\rangle$ is of order $\mathscr{E}^3$. Thus one of the differences between the two-photon and the three-photon (in fact the N-photon with $N>2$) case is that in the former the correction to V_{ca} due to the field is of the same order as the transition to the autoionizing state itself which has some implications about the observability of the effects to be discussed later on. Why the leading correction to V_{ca} is always of order $\mathscr{E}^2$ is also evident from the schematic representation of Fig. 2. The quantity $\tilde{D}_{Eg}^{(3)}(1-i/\tilde{q})$ appearing in Eq. (2.19c) is defined by

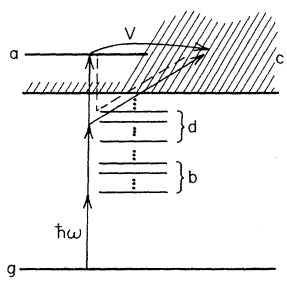

FIG. 2. Schematic diagram for three-photon autoionization.

$$\tilde{D}_{Eg}^{(3)}\equiv\mathscr{E}^3\left[\mu_{ag}^{(3)}+\mathrm{P}\int dE_c\frac{\tilde{V}_{ac}\mu_{cg}^{(3)}}{E-E_c}\right], \tag{2.22a}$$

while $\tilde{q}$ is now given by

$$\tilde{q}\equiv\frac{\tilde{D}_{Eg}^{(3)}}{\pi(\tilde{V}_{ac}\mu_{cg}^{(3)})_{E_c=E}}$$
$$=\frac{\mu_{ag}^{(3)}+\mathrm{P}\int dE_c[\tilde{V}_{ac}\mu_{cg}^{(3)}/(E-E_c)]}{\pi[(V_{ac}+\mathscr{E}^2\mu_{ac})\mu_{cg}^{(3)}]_{E_c=E}}. \tag{2.22b}$$

The meaning and role of these quantities are the same as those of the two-photon case. They only differ in the way they depend on field strength.

Since we have so far been considering a nonresonant (no intermediate resonances) three-photon transition, we can write a transition probability per unit time in the form

$$W^{(3)}=2\pi|D_{cg}^{(3)}|^2\frac{(\epsilon+\tilde{q})^2}{\epsilon^2+1}=2\pi I^3|\mu_{cg}^{(3)}|^2\frac{(\epsilon+\tilde{q})^2}{\epsilon^2+1}, \tag{2.23}$$

with ϵ defined exactly as in Eq. (2.15). This transition probability per unit time is a meaningful quantity as long as $|\tilde{D}_{Eg}^{(3)}|<\Gamma_a$. Otherwise the procedure of Ref. 11 must be employed in calculating ionization as a function of time.

D. Two-photon resonant three-photon autoionization

As noted earlier, there is more than one possibility for resonance in this case. We present a brief summary of equations applicable specifically to one of such cases for which we also report specific calculations, namely, two-photon resonant three-photon ionization. The laser frequency is assumed to be such that $2\omega\cong(E_d-E_g)/\hbar$ where $|d\rangle$ is one of the previously defined intermediate states which can be reached from $|g\rangle$ by a two-photon transition and from which $|a\rangle$ can be reached by a single-photon transition. Assuming that the problem is confined to a frequency range around this particular $|d\rangle$ state, all other states of the type of $|d\rangle$ can be ignored. We have then, similar to that of Sec. II B, a near resonant transition to an intermediate state $|d\rangle$ and a single-photon transition from there to $|a\rangle$ and the respective continuum. The different feature of this case is the matrix element for the transition $|g\rangle\rightarrow|d\rangle$ which now is a two-photon matrix element. We can then rewrite Eqs. (2.16) in exactly the same form with a somewhat modified meaning for some of the symbols. The Rabi frequency Ω_1 is now of second order in $\mathscr{E}$ and is given by

$$\Omega_1^{(2)}=\mathscr{E}^2\mu_{dg}^{(2)}=\mathscr{E}^2\sum_b\frac{\mu_{db}\mu_{bg}}{E_b-E_g-\hbar\omega}. \tag{2.24}$$

For the detuning δ_1 we have $\delta_1=2\hbar\omega-\bar{E}_{bg}$, while the total detuning from the autoionizing state is $\delta=3\hbar\omega-\bar{E}_{ag}$. All other quantities appearing in Eqs. (2.16) retain their definitions and meaning. The overall process is now of third order in $\mathscr{E}$. In the limit of low intensity in which a transition probability per unit time is meaningful, Eqs. (2.17) are still valid with Ω_1 replaced by $\Omega_1^{(2)}$.

The reader may wonder why $\tilde{V}_{ca}$ appears in the equations for the nonresonant cases while the unmodified V_{ca} appears in those for the resonant. The equations for the resonant case contain explicitly the population of the intermediate state. Upon solution of these equations V_{ca} is modified indirectly because it enters the equations in a complicated fashion and not simply as a decay constant. The result for the nonresonant case containing $\tilde{V}_{ca}$ can be obtained from the resonant in the limit of large detuning (or low saturation of the bound-bound transition). Large detuning here is to be understood as larger than the respective Rabi frequency Ω_1 or $\Omega_1^{(2)}$.

In the usual multiphoton resonant ionization, the resonance refers to an intermediate state. Here, in multiphoton resonant autoionization, there is the resonance with the autoionizing state as well. In fact, to talk about autoionization at all, we must assume that the frequency is tuned around this resonance. On the other hand, we may or may not have resonance with an intermediate state. We have therefore two saturations to consider. One has to do with the saturation of the resonant transition to the intermediate state. It occurs when the respective Rabi frequency Ω_1 becomes comparable to or larger than the spontaneous decay of the resonant state $|d\rangle$. The consequences of this type of saturation have been studied in the context of multiphoton ionization, are generally understood, and we shall draw upon those results when necessary. The problem of saturation of the transition to the autoionizing state (either single-photon or two-photon) has also been studied. Saturation here implies (in the notation of this section) $|\tilde{D}_{Eg}|\rangle\Gamma_a$, which for a three-photon transition translates to $|D_{Eg}^{(3)}|\rangle\Gamma_a=\pi|V_{ca}|^2$. Since $\tilde{D}_{Eg}^{(3)}$ is of third order in $\mathscr{E}$, we expect that typically $\tilde{V}_{ca}$ will show departure from V_{ca} before $\tilde{D}_{Eg}^{(3)}$ becomes comparable to Γ_a. In the two photon case the two are apt to occur at about the same intensity.

In summary, we have four types of behavior appearing successively with increasing intensity: Completely nonsaturated autoionization with Γ_a determined by V_{ca} expected at low intensity, saturation of a real near-resonant intermediate state expected even for moderate intensity when the frequency is near resonant with a single-, two-, or multiphoton transition with an intermediate state, modification of V_{ca} at a higher intensity, and finally saturation of the multiphoton autoionizing transition itself at relatively high intensity. The sequence of appearance of these effects (or combinations thereof) depends critically on the particular atom and the frequency of the radiation. In the following sections, the opportunity will be given to illustrate this by referring to specific numerical examples.

III. THREE-PHOTON AUTOIONIZATION OF Sr

A. Derivation of the generalized cross section and angular distribution

We turn now to the application of the preceding formalism and ideas to three-photon autoionization of Sr. In view of the availability of some experimental data we shall emphasize the two-photon resonant situation. The ground state $|g\rangle$ has the configuration $5s^2(^1S_0)$. We are interested in three-photon autoionization to the state $5p6s(^1P_1^o)$ with the possibility of two-photon resonance with states of the configurations $5sns(^1S_0)$, $5snd(^1D_2)$, and in particular the doubly excited states $5p^2(^1S_0)$ and $5p^2(^1D_2)$. We will not be concerned with single-photon resonances from the ground state. Thus we need to sum over intermediate states of the type $5smp(^1P_1)$. In principle, none of such configurations are pure and we must take cognizance of this fact whenever it is quantitatively important. The autoionizing state $|a\rangle=5p6s(^1P_1^o)$ couples and autoionizes to the continuum $5sE_cl$ with $l=1$ at low laser intensities. Coupling of $l=3$ partial wave with $|a\rangle$ due to laser will be studied in a following paper. These two partial waves are those which can be reached from the ground state via three-photon absorption and only $5sE_cp$ interferes in this paper with the transition to $|a\rangle$. The participation of the above states in the total excitation is illustrated in Eq. (3.2) which defines the channels of the transition. Each arrow represents a matrix element of the electric dipole operator. For light of given polarization each matrix element can be written as a radial matrix element multiplied by the appropriate coefficient resulting from the angular momentum algebra. The coefficients shown with each arrow of Eq. (3.2) correspond to light linearly polarized. If the second photon is not in near resonance with any of the accessible states mentioned above, we need to also sum over states of the form $5sns$, $5smd$, and $5p^2$ ($mpnp$, in general). We begin with this completely nonresonant case. Two types of three-photon matrix need be considered: $\mu_{gc}^{(3)}$ and $\mu_{ga}^{(3)}$ each involving two sets of summations. For example, the radial matrix element connecting $|g\rangle=5s^2$ with $|c\rangle=5sE_cp$ involves a sum of the form

$$R_1'\equiv\sum_m\sum_n\frac{\langle 5s^2|r|5snp\rangle\langle 5snp|r|5sms\rangle\langle 5sms|r|5sE_cp\rangle}{(E_n-E_g-\hbar\omega)(E_m-E_g-2\hbar\omega)}\,, \tag{3.1}$$

which we abbreviate as

$$5s^2\xrightarrow{1/\sqrt{3}}5snp\xrightarrow{1/\sqrt{3}}5sms\xrightarrow{1/\sqrt{3}}5sE_cp\,,$$

with the angular momentum factors also indicated above the arrow. Thus R_1' must be multiplied by the product

$$\frac{1}{\sqrt{3}}\frac{1}{\sqrt{3}}\frac{1}{\sqrt{3}}$$

of these coefficients before it is entered in an expression for the transition amplitude because the defining equation (3.1) contains only radial matrix elements. With the above notation in mind, we define the following effective

(three-photon) matrix elements:

$$
\begin{aligned}
R_1' &\equiv 5s^2 \xrightarrow{1/\sqrt{3}} 5snp \xrightarrow{1/\sqrt{3}} 5sms \xrightarrow{1/\sqrt{3}} 5sE_cp\ , \\
R_1 &\equiv 5s^2 \xrightarrow{1/\sqrt{3}} 5snp \xrightarrow{1/\sqrt{3}} 5sms \xrightarrow{1/\sqrt{3}} 5p6s\ , \\
R_2' &\equiv 5s^2 \xrightarrow{1/\sqrt{3}} 5snp \xrightarrow{2/\sqrt{15}} 5smd \xrightarrow{2/\sqrt{15}} 5sE_cp\ , \\
R_2 &\equiv 5s^2 \xrightarrow{1/\sqrt{3}} 5snp \xrightarrow{2/\sqrt{15}} 5smd \xrightarrow{2/\sqrt{15}} 5p6s\ , \\
R_3 &\equiv 5s^2 \xrightarrow{1/\sqrt{3}} 5snp \xrightarrow{2/\sqrt{15}} 5smd \xrightarrow{3/\sqrt{35}} 5sE_cf\ , \\
R_4' &\equiv 5s^2 \xrightarrow{1/\sqrt{3}} 5snp \xrightarrow{1/\sqrt{3}} 5p^2(^1S_0) \xrightarrow{1/\sqrt{3}} 5sE_cp\ , \\
R_4 &\equiv 5s^2 \xrightarrow{1/\sqrt{3}} 5snp \xrightarrow{1/\sqrt{3}} 5p^2(^1S_0) \xrightarrow{1/\sqrt{3}} 5p6s\ , \\
R_5' &\equiv 5s^2 \xrightarrow{1/\sqrt{3}} 5snp \xrightarrow{1/\sqrt{3}} 5p^2(^1D_2) \xrightarrow{1/\sqrt{3}} 5sE_cp\ , \\
R_5 &\equiv 5s^2 \xrightarrow{1/\sqrt{3}} 5snp \xrightarrow{1/\sqrt{3}} 5p^2(^1D_2) \xrightarrow{1/\sqrt{3}} 5p6s\ .
\end{aligned}
\tag{3.2}
$$

In addition to the three-photon matrix elements that excite the atom above the $5sE_cl$ threshold, we need the two-photon matrix element $\mu_{ac}^{(2)}$ coupling the autoionizing state to its continuum and modifying V_{ac}. It involves a summation over states $5sms$, $5smd$, $5p^2(^1S_0)$, and $5p^2(^1D_2)$ as intermediate states. Keeping with our notation, we define the quantities

$$
\begin{aligned}
Q_1 &\equiv 5p6s \xrightarrow{1/\sqrt{3}} 5sms \xrightarrow{1/\sqrt{3}} 5sE_cp\ , \\
Q_2 &\equiv 5p6s \xrightarrow{2/\sqrt{15}} 5smd \xrightarrow{2/\sqrt{15}} 5sE_cp\ , \\
Q_2' &\equiv 5p6s \xrightarrow{2/\sqrt{15}} 5smd \xrightarrow{3/\sqrt{35}} 5sE_cf\ , \\
Q_3 &\equiv 5p6s \xrightarrow{1/\sqrt{3}} 5p^2(^1S_0) \xrightarrow{1/\sqrt{3}} 5sE_cp\ , \\
Q_4 &\equiv 5p6s \xrightarrow{1/\sqrt{3}} 5p^2(^1D_2) \xrightarrow{1/\sqrt{3}} 5sE_cp\ ,
\end{aligned}
\tag{3.3}
$$

which imply summation over m as in Eq. (3.1).

Now let $M_{Eg}^{(3)}$ be the overall transition amplitude from the initial state to the modified continuum state Ψ_E. This amplitude can be written in terms of the quantities defined above and the spherical harmonics corresponding to the final state of the outgoing photoelectron. In a system of spherical coordinates where the z axis is taken along the polarization vector of the linearly polarized radiation and the x axis along the direction of propagation, the photoelectron wave vector $\vec{K}$ is defined in terms of its coordinates (K,Θ,Φ), and $M_{Eg}^{(3)}$ is expressed in terms of spherical harmonics of the unit vector $\hat{K}$. The bound-free radial matrix elements are multiplied by the appropriate factor $e^{-i\delta_l}$ where δ_l is the phase shift of the lth partial wave.

The transition matrix element $M_{Eg}^{(3)}$ can now be put in the form

$$
M_{Eg}^{(3)} = -\sqrt{4\pi} i e^{i\delta_1}[A_1 P_1(\cos\Theta) - A_3 e^{-i\delta_{1,3}} P_3(\cos\Theta)]\ ,
\tag{3.4}
$$

where $P_l(x)$ are Legendre polynormals, δ_{13} is the difference $\delta_1-\delta_3$ of the phase shifts, and A_1 and A_3 are defined by

$$
A_1 = \tfrac{1}{3}(R_1+\tfrac{4}{5}R_2+\tfrac{1}{3}R_4+\tfrac{2}{3}R_5)\frac{\sin\Delta}{\pi(V_{ca}+D_{ca}^{(2)})} - (R_1'+\tfrac{4}{5}R_2'+\tfrac{1}{3}R_4'+\tfrac{2}{3}R_5')\cos\Delta\ ,
\tag{3.5a}
$$

$$
A_3 = \tfrac{2}{5}R_3\ ,
\tag{3.5b}
$$

where

$$
D_{ca}^{(2)} = \frac{2\pi\alpha\omega I}{3}(Q_1+\tfrac{4}{5}Q_2+\tfrac{1}{3}Q_3+\tfrac{2}{3}Q_4)\ .
\tag{3.5c}
$$

We will leave the investigation of the effect of Q_2' in a more complete treatment of this coupled-continua problem to a following paper. The differential cross section for photoelectron emission within the solid angle $d\Omega$ and hence the photoelectron angular distribution, is determined by $|M_{Eg}^{(3)}|^2$, which after some algebraic manipulation leads to

$$
\frac{d\hat{\sigma}_3}{d\Omega} = \frac{8\pi}{(2\pi\alpha\omega)^3}\frac{\hat{\sigma}_3}{4\pi}(\beta_2\cos^2\Theta+\beta_4\cos^4\Theta+\beta_6\cos^6\Theta)\ ,
\tag{3.6}
$$

where

$$
\beta_2 \equiv A_1^2+\tfrac{9}{4}A_3^2+3A_1A_3\cos\delta_{13}\ ,
\tag{3.7a}
$$

$$
\beta_4 \equiv -\tfrac{15}{2}A_3^2-5A_1A_3\cos\delta_{13}\ ,
\tag{3.7b}
$$

$$
\beta_6 \equiv \tfrac{25}{4}A_3^2\ .
\tag{3.7c}
$$

Integration over $d\Omega$ leads to the total generalized cross section for three-photon autoionization given by

$$
\hat{\sigma}_3 = \frac{(2\pi\alpha\omega)^3(4\pi)^2}{8\pi}(\tfrac{1}{3}A_1^2+\tfrac{1}{7}A_3^2)\ .
\tag{3.8}
$$

The atomic structure information is contained in the coefficients R_i and Q_i. The latter are involved in the calculation of $D_{ca}^{(2)}$ which, as we have shown in Sec. II, contains the influence of the intensity on V_{ca}. Note that Eq. (3.5) contains trigonometric functions of Δ which is given by

$$
\Delta = -\tan^{-1}\left[\frac{\pi|V_{ca}+D_{ca}^{(2)}|^2}{E-E_a-F_a}\right]\ ,
\tag{3.9}
$$

the usual expression in autoionization. Here, however, instead of simply V_{ca} we have the intensity-dependent $\tilde{V}_{ca}=V_{ca}+D_{ca}^{(2)}$ appearing in all expressions.

B. Calculation of matrix elements and channel transition amplitudes

For each of the channels defined in Eqs. (3.2) and (3.3) we need representations for the wave functions as well as execution of the infinite summations. All wave functions must be properly antisymmetrized and all matrix elements will involve the two-electron operator $\vec{r}_\alpha+\vec{r}_\beta$. When the two-electron wave functions are expressed as an antisymmetrized linear combination of products of single-electron

wave functions, a transition matrix element in two-electron space reduces to one or two single-electron transition matrix elements multiplied by a factor representing the overlap of the initial and final wave functions of the other electron. Depending on the calculational model, this factor can be unity. The summation over the intermediate states of the type $5snp$, $5sms$, and $5smd$ is carried out by means of a single-particle quantum-defect Green's function. Recall that a summation of the type

$$\sum_n \frac{\langle b \mid \vec{r} \mid n \rangle \langle n \mid \vec{r} \mid a \rangle}{(E_n - E_a - \hbar\omega)}$$

can be written exactly as

$$\int d^3r_2 \int d^3r_1 \, \psi_b(\vec{r}_2)\vec{r}_2 G(\vec{r}_2,\vec{r}_1;\Omega)\vec{r}_1\psi_a(\vec{r}_1)$$

if the Green's function G or a satisfactory approximation thereof is known. For wave functions corresponding to a central field, we can define "radial" Green's functions g_l, pertaining to a particular angular momentum, by separating out the angular parts. From the defining equation

$$G(\vec{r}_2,\vec{r}_1;\Omega) \equiv \sum_n \frac{\Psi_n^*(\vec{r}_2)\Psi_n(\vec{r}_1)}{E_n - \hbar\Omega} , \tag{3.10}$$

with $\hbar\Omega$ being an arbitrary energy, we define g_l through the equation

$$G(\vec{r}_2,\vec{r}_1;\Omega) \equiv \sum_{l,m} \frac{g_l(r_1,r_2;\Omega)}{r_1 r_2} Y_{lm}^*(\hat{r}_2) Y_{lm}(\hat{r}_1) , \tag{3.11}$$

where $\hat{r}_j$ are unit vectors along $\vec{r}_j$. It is the selection rule for dipole transitions that determines which terms survive in the double sum over lm. A double summation over intermediate states will involve a product of two Green's functions, etc.

Let us consider now, as an example, the channel amplitude R_1'. We have a two-electron initial state $\psi_{5s^2}(\vec{r}_1,\vec{r}_2)$ to be understood as a product of two single-electron wave functions denoted by $\psi_{5s^2}(\vec{r}_j)$. We also have a $5s$ wave function appearing in the final state $5sE_cp$ which corresponds to the ground state of the ion and will be denoted by $\psi_{5s}(\vec{r})$. In general, depending on the model, ψ_{5s^2} is not the same as ψ_{5s}.

At the same time, a ψ_{5s} state occurs in the representation of the excited states $5snl$. Although, in general, every nl requires a slightly different $5s$, we assume here one and the same ψ_{5s}. In calculating a matrix element of the form $\langle 5smp \mid \vec{r}_\alpha + \vec{r}_\beta \mid 5s^2 \rangle$ between antisymmetrized wave functions, we obtain products of the form $\langle \psi_{mp}(\vec{r}_\alpha) \mid \vec{r}_\alpha \mid \psi_{5s^2}(\vec{r}_\alpha) \rangle \langle \psi_{5s}(r_\beta) \mid \psi_{5s^2}(\vec{r}_\beta) \rangle$ where the second (overlap) factor is different from unity. From another viewpoint, it reflects the fact that $5s^2$ is not a pure configuration, but contains admixtures of other configurations as well. Since we are dealing with singlet states, the spatial wave functions will be symmetric with respect to spatial coordinates and, consequently, the two-electron wave function $5snp$ is written as $(1/\sqrt{2})[\psi_{5s}(\vec{r}_\alpha)\psi_{mp}(\vec{r}_\beta) + \psi_{5s}(\vec{r}_\beta)\psi_{mp}(\vec{r}_\alpha)]$, etc. With this notation for wave functions, we can now write R_1' as

$$R_1' = \int dr_1 \int dr_2 \int dr_3 \left[\psi_{E_cp}^*(r_3) r_3 g_0(r_3,r_2;\Omega_2) + \psi_{5s}^*(r_3) g_0(r_3,r_2;\Omega_2) \int dr \, \psi_{E_cp}^*(r) r \psi_{5s}(r)\right]$$
$$\times \left[r_2 g_1(r_2,r_1;\Omega_1) + \psi_{5s}(r_2) \int dr \, \psi_{5s}^*(r) r g_1(r,r_1;\Omega_1)\right] r_1 \psi_{5s^2}(r_1) \sqrt{2} \int dr \, \psi_{5s}^*(r) \psi_{5s^2}(r) , \tag{3.12}$$

where $\psi(r)$ is to be understood here as the radial part of the wave function multiplied by r. In a similar fashion, we write the Q's in terms of a Green's function, as, for example,

$$Q_1 = \int dr_1 \int dr_2 \psi_{E_cp}^*(r_2) r_2 g_0(r_1,r_2;\Omega_2) \left[\psi_{6s}(r_1) \int dr \, \psi_{5s}^*(r) r \psi_{5p}(r) + r_1 \psi_{5p}(r_1) \int dr \, \psi_{5s}^*(r) \psi_{6s}(r)\right] . \tag{3.13}$$

The parentheses contain two terms because in the channel represented by Q_1 we have states of the form $5sns$ as intermediate states in which both electrons can be connected through a dipole transition to an mp or an E_cp state. The overlap $\langle 5s \mid 6s \rangle$ has been retained as nonvanishing because, as noted earlier, $5s$ refers to the core of the doubly ionized atom, while $6s$ refers to a "$5p$+core" potential. All Green's functions above are evaluated at the appropriate energy, which means $E_g + \hbar\omega$ or $E_g + 2\hbar\omega$ depending on whether it represents summation over the first or second set of intermediate states. For example, $\hbar\Omega_2 = E_g + 2\hbar\omega$ and $\hbar\Omega_1 = E_g + \hbar\omega$ in Eq. (3.12). All other R's and Q's are given by similar expressions differing in the final state and/or Green's function. Thus R_2 involves $5p6s$ as final state and $g_2(r_3,r_2;\Omega_2)$ instead of $g_0(r_3,r_2;\Omega_2)$ with only one term in each square bracket [see Eq. (3.12)] since in this channel we have intermediate states of the type $5snd$ instead of $5sns$. It explicit form then is

$$R_2 = \int dr \, \psi_{6s}^*(r)\psi_{5s}(r) \int dr_1 \int dr_2 \int dr_3 \psi_{5p}^*(r_3) r_3 g_2(r_3,r_2;\Omega_2) r_2 g_1(r_2,r_1;\Omega_1) r_1 \psi_{5s^2}(r_1)\sqrt{2} \int dr \, \psi_{5s}^*(r)\psi_{5s^2}(r) . \tag{3.14}$$

The Green's function employed in our calculations are expressed in terms of the quantum defects of the respective series of intermediate states and the Whittaker function. Formal expressions for these Green's functions can be found elsewhere. When the second photon involves $5p^2$ as an intermediate state, no Green's function intervenes at that step which must be handled separately with that particular single intermediate state. This is the case with channels R_4, R_4', R_5, R_5', Q_3, and Q_4. Strictly speaking these correspond to the truncation of the infinite summation over states of the form $npmp$ to a single term which in this paper plays the dominant role owing to the near

resonance with the energy of two photons.

Finally, the formal expression for the continuum wave function of the l partial wave is

$$\Psi_{E_c l}(\vec{r})=4\pi i^l e^{-i\delta_l} G_{Kl}(r) \sum_{m=-l}^{l} Y_{lm}(\theta,\phi) Y_{lm}^*(\Theta,\Phi) , \tag{3.15}$$

where $G_{Kl}(r)$ has been calculated numerically in all of the results reported in this paper. The continuum enters in the calculation of electric dipole matrix elements as well as matrix elements of V, as in V_{ca}, which often imposes different demands on the calculation of the wave function as discussed in Sec. III C.

C. Calculation of wave functions and configuration interaction

We have already seen that the intermediate states $5snp$, $5sms$, and $5smd$ are summed over via the single-channel quantum-defect Green's function. This, however, does not mean that configuration mixing is totally lost in the transition. It appears indirectly through the overlaps $\langle 5s \mid 5s^2 \rangle$, $\langle 5s \mid 6s \rangle$, etc., of the single-particle wave functions. These overlaps are nonvanishing because of the way our wave functions are calculated. The initial state $(1s^2-4p^6)5s^2\,{}^1S$ is calculated in a single configuration using a multiconfiguration Hartree-Fock program (MCHF).[14] The doubly excited states $5p^2\,{}^1S$, $5p^2\,{}^1D$, and $5p6s\,{}^1P$ are calculated with the core part $(1s^2-4p^6)$ frozen in single configurations in MCHF. The ionic ground state $(1s^2-4p^6)5s$ is also calculated in the same frozen core, and this $5s$ wave function is used in constructing the singly excited intermediate states $5sml$. The continuum states $5sE_cp\,{}^1P$ and $5sE_cf\,{}^1F$ are continuum numerical solutions in the potential of $(1s^2-4p^6)5s$ and are normalized per unit energy, i.e.,

$$u_{El}(r)\sim \left[\frac{2}{\pi K}\right]^{1/2} \sin\left[Kr-\frac{l\pi}{2}+\frac{\ln(2Kr)}{K}+\delta_l\right] \quad \text{for } r\to\infty .$$

Given that our wave functions have the above-mentioned nonvanishing overlaps, V is not simply $1/r_{12}$ as in other calculational schemes. Since we employ wave functions that "see" different potentials, part of $1/r_{12}$ is already included and allowance must be made for its contribution. To this end we study V_{ca}, the configuration interaction between the discrete configuration $\mid a \rangle = 5p6s\,{}^1P$ and the continuum $\mid c \rangle = 5sEp$ separately. We consider the matrix element $V_{ca}=\langle 5sEp\,{}^1P \mid H \mid 5p6s\,{}^1P \rangle$ in a model Hamiltonian which we write as

$$H=h_1+h_2+\frac{1}{r_{12}} ,$$

where $h_i=(P_i^2/2m)-(Z_{\text{eff}}/r_i)$ with Z_{eff} being used as a parameter. V_{ca} turns out to be rather sensitive to the value of Z_{eff} as can be recognized in Table I. A better approximation can be obtained by letting Z_{eff} become a function of r, thus taking into account the inner and outer screening due to the core electrons. Thus we take

$$Z_{\text{eff}}(r)=\sum_{nl=1s}^{4p} a_{nl}\left[\int_0^r u_{nl}^*(r')u_{nl}(r')dr' + \int_r^\infty \frac{r}{r'} u_{nl}^*(r')u_{nl}(r')dr'\right] ,$$

where $n=1,2,3,4$ and $a_{nl}=2,6,10$ for $l=0,1,2$, respectively. Now as r increases from 0 to ∞, Z_{eff} varies from 38 to 2 and the resulting value of V_{ca} is 5×10^{-2}, while the matrix element $\langle c \mid 1/r_{12} \mid a \rangle$ is 5.9×10^{-2}. One can attempt to subtract the overestimated part of V since V should be the difference between $1/r_{12}$ and the part of the interaction between the two valence electrons which is already taken into account in the self-consistent potential employed in the calculation of the wave functions. A typical result of such attempts is

$$\left\langle 5sEp\left|\frac{1}{r_{12}}\right|5p6s\right\rangle-\left\langle Ep\left|\frac{\int_0^r u_{5s}^*(r)u_{6s}(r)dr}{r}\right|5p\right\rangle = 4\times10^{-2} ,$$

which could be taken as the square root of the width of $5p6s\,{}^1P_1^o$ if it were an isolated resonance. High resolution data do not exist in that region. The existing single-photon absorption data show a rather complex structure which points to strong interference of $5p6s\,{}^1P_1^o$ with the state $4d(^2D_{5/2})4f[\frac{1}{2}]_1^o$. Thus in a single-photon experiment it is not possible and probably not meaningful to assign a width to the $5p6s$ resonance. On the other hand, the resonance may appear more pronounced in a multiphoton experiment owing to intensity effects. Some evidence in that direction appears in the multiphoton data. It would be premature to say that we are dealing with an intensity effect. But it is definitely true that the broad structure of single-photon absorption separates into rather well-separated peaks when excited via three-photon absorption. One of those peaks appears approximately where the $5p6s\,{}^1P_1^o$ should be. A complication arises from the persistence of this peak under excitation with circularly polarized light as well, which points to the presence of total angular momentum 3. A significant contribution from the state $5p6s\,{}^1P_1^o$ should, however, be present in any case. We adopt then the following program. We study the resonance $5p6s\,{}^1P_1^o$ as isolated, we calculate the intensity effects, and in a follow-up paper we address the question of interference with other resonances and examine how a separation of resonances can occur under multiphoton excitation.

For the present calculation, we estimate the width of the $5p6s\,{}^1P_1$ resonance from the uv absorption spectrum[15] as being about 70 cm^{-1} which correspond to a value of

TABLE I. Study of V_{ca} in a model Hamiltonian of $H=h_1+h_2+1/r_{12}$, where $h_i=(P_i^2/2m)-(Z_{\text{eff}}/r_i)$.

Z_{eff}	2.0	2.5	5.3	5.4	5.5	5.6	5.8	7.0
V_{ca}	1.5×10^{-1}	1.3×10^{-1}	1.3×10^{-2}	8.6×10^{-3}	4.5×10^{-3}	4.4×10^{-4}	-7.8×10^{-3}	-5.7×10^{-2}

$|V_{ca}|$ about 7×10^{-3} a.u. In view of the experimental uncertainties, this has to be viewed as an order-of-magnitude estimate. The sign of V_{ca} is taken to be positive to be consistent with our model calculations. The sign is important in the investigation of laser-intensity effects [see Eq. (2.7), or (3.5) with (3.9)].

D. Results and discussion

In this section we present samples of results from three types of calculations: Three-photon generalized cross sections, resonance line shapes (including the effect of ac Stark shifts), and photoelectron angular distributions. The effect of laser intensity on all of these aspects of the process has been calculated at each stage.

Beginning with the total generalized three-photon ionization cross section, we note that owing to the presence of intermediate as well as autoionizing resonances, we expect a sensitive dependence on laser frequency throughout the range of frequencies considered in this paper. This sensitivity is evident in Figs. 3–5. Before elaborating on the details of these figures, let us observe that the order of magnitude of $\hat{\sigma}_3$ near resonance is about 5×10^{-75} $\text{cm}^6\,\text{sec}^2$ which represents a rather high generalized cross section for a three-photon process. To put this magnitude in an experimental context, note that a laser intensity of $\sim10^9$ W/cm^2 in this frequency range corresponds to a photon flux F of about 3×10^{27} photons/cm^2 sec. This would give a transition probability per unit time $F^3\hat{\sigma}_3\cong10^8$ sec^{-1} which means that with a pulse duration

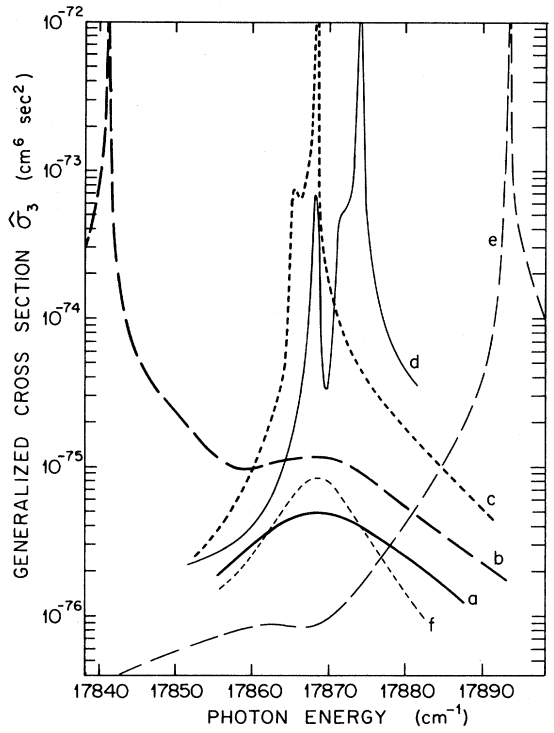

FIG. 4. Same as Fig. 3 with $5s5d$ state ac Stark shift of (1 cm)/(10^{27}/cm^2 sec) included. *a*, low-intensity limit, same as *a* in Fig. 3; *b*, $I=9.54\times10^{29}$ photons/cm^2 sec; *c*, $I=1.008\times10^{30}$; *d*, $I=1.024\times10^{30}$; *e*, $I=1.059\times10^{30}$; *f*, $I=4.35\times10^{30}$.

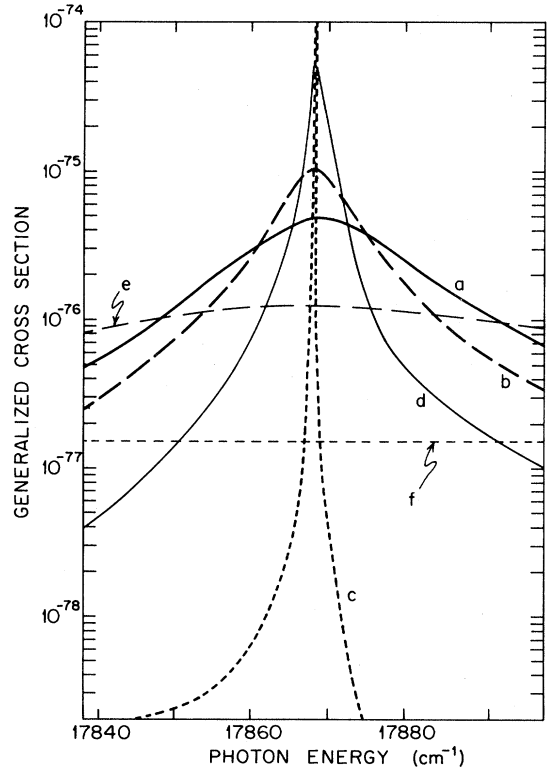

FIG. 3. Three-photon autoionization of Strontium near $5p6s\ ^1P$ resonance without ac Stark shift. *a*, low-intensity limit; *b*, $I=5.5\times10^{30}$ photons/cm^2 sec; *c*, $I=1.1\times10^{31}$; *d*, $I=2.2\times10^{31}$; *e*, $I=4.95\times10^{31}$; *f*, $I=1.1\times10^{32}$.

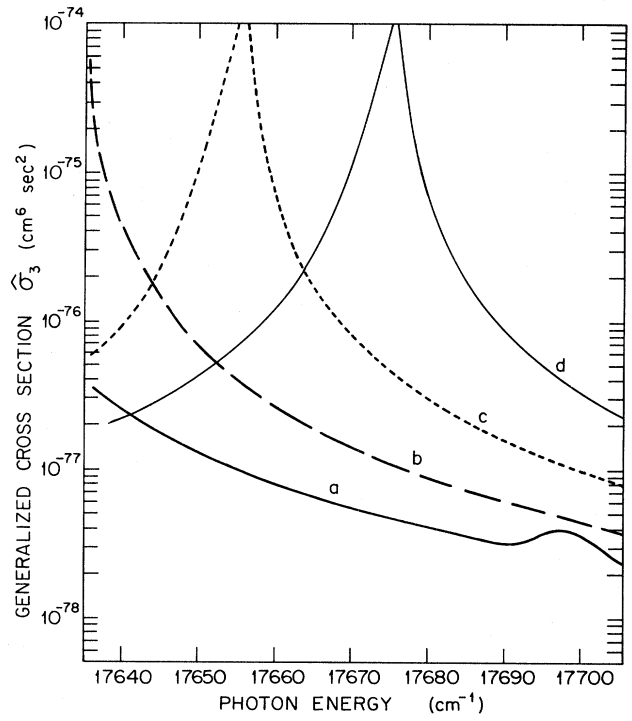

FIG. 5. Same as Fig. 3 with ac Stark shifts of (1 cm)/(10^{27}/cm^2 sec) for $5s5d$ and (-1 cm)/(10^{27}/cm^2 sec) for $5p6s$ included. *a*, $I=5.0\times10^{27}$ photons/cm^2 sec; *b*, $I=5.4\times10^{27}$; *c*, $I=5.8\times10^{27}$; *d*, $I=6.2\times10^{27}$.

T_L of about 5—10 nsec, the ionization probability per pulse ($F^3\hat{\sigma}_3 T_L$) is close to unity. This explains to a large extent the copious amount of Sr^+ observed in related experiments. At the frequency range around the second harmonic of the Nd laser (about 18 790 cm^{-1}), total ionization should have taken place. On the basis of this evidence alone, it might seem that Sr^{2+} also observed in the experiments was produced through ionization of Sr^+ which is an alkalilike ion. This requires a five-photon ionization process whose generalized cross section we have estimated through a truncated summation calculation, with the result $\hat{\sigma}_5 \simeq 10^{-139}$ $cm^{10}sec^4$. For a photon flux 3×10^{27}, as above, we would have $\hat{\sigma}_5 F^5 \cong 2.43\times10^{-2}$ sec^{-1} and for $T_L = 10$ nsec, $\hat{\sigma}_5 F^5 T = 2.43\times10^{-10}$ which implies that only 10^{-10} of the atoms Sr^+ ions would have been ionized during the laser pulse. This number would suggest a rather small yield of Sr^{2+} contrary to the experimental observation which showed large yield, close to saturation. Our estimate cannot be taken literally. The value of $\hat{\sigma}_5$ could easily be off by 2 or 3 orders of magnitude, and if the experimental intensity is underestimated by a factor of 10, the signal is off by a factor of 10^7 or 10^8. We cannot, therefore, say more about Sr^{2+} until a more accurate experimental number becomes available, in which case a calculational effort for a more reliable theoretical estimate will be justifiable. It is worth noting at this point, however, that new recent preliminary results have shown small Sr^{2+} but large Sr^{3+} yields almost comparable to Sr^+.[16] This is new evidence compatible with our conjecture that there is significant involvement of transitions between autoionizing states which we will address in a follow-up paper.

Let us return now to the resonance aspects of Figs. 3—5 and consider first the behavior around the $5p6s(^1P)$ autoionizing resonance without including the ac Stark shifts. As the intensity changes, the dominant expected effect, in the absence of such shifts, is the line distortion due to the modification of V. This is demonstrated in the sequence of curves from a—e in Fig. 3 which show a transition from a line about 23 cm^{-1} wide (curve a) to an extremely narrow (curve c) and then to a wide curve (e) as the intensity changes by about 2 orders of magnitude. The most dramatic change appears at about 10^{31} photons/cm^2 which corresponds to 3×10^{12} W/cm^2.

We turn next to Fig. 4 which shows the autoionization signal around the same resonance $5p6s(^1P)$ but with the ac Stark shift for the nearest $5s5d$ intermediate state included. The magnitude of this shift is about 1 cm^{-1} per 10^{27} photons/cm^2 sec of photon flux. Again, at low intensity (curve a) we have the bare resonance as in Fig. 3. The $5s5d$ is outside the width of the resonance. As the intensity increases, $5s5d$ begins to move towards the center eventually coming into resonance with the photon frequency that also corresponds to three-photon resonance with the autoionizing state. This occurs somewhere around the intensity of curve c. The sharp resonance of curve b corresponds to the two-photon resonance with $5s5d$ which, with increasing intensity, shifts to the right of the autoionizing resonance as in curves d and f. Superimposed on this shifting of the intermediate state is the narrowing of the autoionizing resonance illustrated in Fig. 3. At the intensity for which the two resonances coincide, the line shape is the result of both effects which strictly speaking cannot be separated because they interfere. It is only for the sake of illustration of their respective magnitudes that are here calculated and discussed in successive approximations. For the same reason, we have not included the ac Stark shift of the autoionizing resonance $5p6s$ in the previous two figures. It is found to be approximately equal to that of the $5snd$ but of opposite sign and its effect is shown in Fig. 5 which includes all three intensity effects. The total effect is quite dramatic, not only because of the significant distortion of the line shape but more importantly because of the different range of intensity at which it occurs when ac Stark shifts combine with the modification of V. As we go from Fig. 3 to Fig. 5, we find the line distortion occurring at intensities 2 orders of magnitude lower. Note that according to Fig. 5, the autoionizing resonance would begin undergoing severe distortion at intensities about 10^{10} W/cm^2. It bears repeating that the Stark shifts do not appear as simple superpositions interfering with the effect of $D_{ca}^{(2)}$ in a linear fashion. They, in fact, enhance $D_{ca}^{(2)}$ by bringing one intermediate state closer to resonance. Thus in Fig. 5, for example, we not only have the eventual merging of two resonances but also the substantial impact of the ac Stark shifts on the two-photon matrix element $D_{ca}^{(2)}$.

The above changes of the resonance behavior with laser intensity are usually expected to produce corresponding changes in the angular distribution of the emitted photoelectrons. This would result mainly from the changes in the relative weight of the participating channels as the resonances shift with respect to each other. A calculation illustrating this effect has produced the results shown in Fig. 6. The angular distributions shown in this figure correspond to a photon frequency such that $E_g + 3\hbar\omega$ is at the peak of the $5p6s(^1P)$ resonance at low intensity. The changes of the distribution (from a—f) occur as the photon flux varies from 1.0—4.35×10^{30} photons/cm^2 sec. The calculation includes the shift of the intermediate state $5s5d$ but not the shift of $5p6s$. The effect seen in these changes therefore represents the variation of channel superposition as $5s5d$ shifts towards the autoionizing resonance. This figure is the counterpart of Fig. 4, in the sense that each angular distribution corresponds to one line-shape curve of Fig. 4. The inclusion of the Stark shift of the autoionizing resonance would lead to a different angular distribution for a particular intensity, but

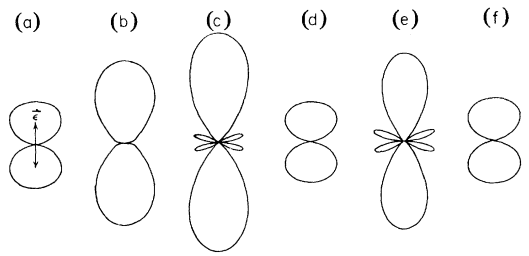

FIG. 6. Angular distributions of the photoelectrons at the peak position of $5p6s\ ^1P$. ac Stark shift of (1 cm)/(10^{27}/cm^2 sec) for $5s5d$ state is included. (a) low-intensity limit, (b) $I = 1.0\times10^{30}$ photons/cm^2 sec, (c) $I = 1.008\times10^{30}$, (d) $I = 1.016\times10^{30}$, (e) $I = 1.059\times10^{30}$, (f) $I = 4.35\times10^{30}$.

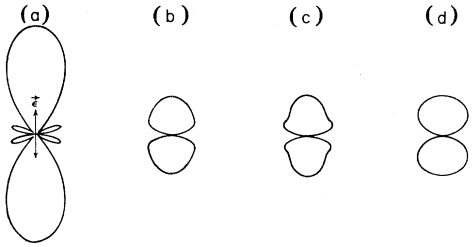

FIG. 7. Calculated angular distributions of photoelectrons from three-photon ionization of Sr with intermediate $5s5d\ ^1D$ resonance. The summation over the first (nonresonant $5snp$) intermediate states is handled with quantum-defect Green's function, and the second (resonant) intermediate states are calculated differently in four cases: (a) Truncated to 1 state—single-configuration $5s5d\ ^1D$ state wave function by MCHF[14] with $(1s-5s)$ electrons frozen in ground configuration of Sr^+. (b) Truncated to 1 state—quantum-defect $5d$ wave function. (c) Single-particle Green's function for all three channels $(5s^2\rightarrow\rightarrow 5sns\rightarrow 5s\epsilon p$, $5s^2\rightarrow\rightarrow 5snd\rightarrow 5s\epsilon p$, and $5s^2\rightarrow\rightarrow 5snd\rightarrow 5s\epsilon f)$. (d) Truncated to 1 state—$5d$ wave function calculated in a modified Hartree-Fock-type potential. The ratios of the transition amplitude (except for $i^{-l}e^{i\delta_l}$) $S_{\epsilon f}/S_{\epsilon p}$ are 3.5, −0.44, −0.55, and −0.13 for (a), (b), (c), and (d), respectively.

the sequence of changes would be roughly the same. The phenomenon depicted in this figure is reminiscent of a similar effect predicted for three-photon ionization (not autoionization) of Na (Ref. 17) and observed in recent experiments.[18]

The above discussion of the angular distribution focused upon the laser-intensity effect. We turn now to an equally important aspect: The dependence of the distribution on the atomic model. In Fig. 7 we show the angular distribution for three-photon ionization through two-photon resonance with the $5s5d$ intermediate state. The photon energy is such that $2\hbar\omega=E_{5s5d}-E_{5s^2}$. At weak intensity, $3\hbar\omega$ is far from an autoionizing state. The resulting angular distribution therefore reflects the properties of $5s5d$ and the continuum to which it ionizes, namely, $5s\epsilon p$ and $5s\epsilon f$. The calculated distributions shown in Fig. 7 test how well the four different schemes employed in the calculation reproduce the observed data.[3] It is one of the quantum-defect calculations that gives better agreement, although one might have expected the calculation of Fig. 7(a) to have been closer to the experiment which shows distinct lobes in the distribution. The main difference between Fig. 7(a) and Figs. 7(b)—7(d) can be traced to the existence of a Cooper minimum (zero of the radial matrix element) in the $5d\rightarrow\epsilon f$ channel near the photon energy of the experiment. The position of the minimum is sensitive to the atomic wave function. If the minimum falls at the photon energy in the continuum, the f channel does not contribute and the distribution from the remaining p channel exhibits no lobe. A pure f-channel contribution, on the other hand, would give a distribution with two pronounced lobes resembling that of Fig. 7(a). If the photon energy falls somewhat away from the minimum, but the f channel does not dominate, the resulting interference between the p and f channels will tend to make the lobes less prominent resembling those of the experiment[3] and of Fig. 7(c). Owing to the rather limited available data, we cannot make more detailed comparisons at this time. The left-right asymmetry exhibited by the data cannot be understood in the context of interaction of an unoriented atom with light of a single polarization and must be sought in instrumental aspects. We close this discussion with the observation that the angular distribution is sensitive to the atomic model and offers interesting possibilities for meaningful interplay of theory with experiment.

The illustrative calculations summarized in this section are but a small sample of the types of behavior apt to be encountered in multiphoton autoionization. We have concentrated on the intensity effect upon a single autoionizing resonance and the associated influence of the ac Stark shifts. As usual, this constitutes one part of a larger picture which must include interaction between autoionizing resonances and the modification thereof by the laser intensity, mixing of continua because of the large intensity, multiconfiguration calculation of autoionizing, as well as intermediate states and their modification by the laser intensity. These aspects which will be the subject of forthcoming papers are necessary for the understanding of transitions between autoionizing states or, more generally, transitions within the continuum.

ACKNOWLEDGMENTS

We are grateful to Professor Tu-nan Chang for many helpful conversations. This work is supported by the National Science Foundation under Grant No. PHY-81-00251.

[1]I. S. Aleksakhin, N. B. Delone, I. P. Zapesochny, and V. V. Suran, Zh. Eksp. Teor. Fiz. 76, 887 (1979) [Sov. Phys.—JETP 49, 447 (1979)].
[2]D. Feldmann, J. Krautwald, S. L. Chin, A. von Hellfeld, and K. H. Welge, J. Phys. B 15, 1663 (1982).
[3]D. Feldmann and K. H. Welge, J. Phys. B 15, 1651 (1982).
[4]A. L'Huillier, L. A. Lompre, G. Mainfray, and C. Manus, Phys. Rev. Lett. 48, 1814 (1982).
[5]T. S. Luk, H. Pummer, K. Boyer, M. Shahidi, H. Egger, and C. K. Rhodes, Phys. Rev. Lett. 51, 110 (1983).
[6]Young Soon Kim and P. Lambropoulos, Phys. Rev. Lett. 49, 1698 (1982).
[7]K. Rai Dastidar and P. Lambropoulos, Chem. Phys. Lett. 93, 273 (1982); Phys. Rev. A 29, 183 (1984).
[8]P. Lambropoulos, Appl. Optics 19, 3926 (1980).
[9]P. Lambropoulos and P. Zoller, in *Multiphoton Ionization of Atoms,* edited by S. L. Chin and P. Lambropoulos (Academic, New York, in press).
[10]U. Fano, Phys. Rev. 124, 1866 (1961).
[11]P. Lambropoulos and P. Zoller, Phys. Rev. A 24, 379 (1981).
[12]K. Rzazewski and J. H. Eberly, Phys. Rev. Lett. 47, 408 (1981).
[13]G. S. Agarwal, S. L. Haan, K. Burnett, and J. Cooper, Phys. Rev. Lett. 48, 1164 (1982).

[14]C. F. Fischer, Comput. Phys. Commun. 4, 107 (1972).
[15]W. R. S. Garton, G. L. Grasdalen, W. H. Parkinson, and E. M. Reeves, J. Phys. B 1, 114 (1968).
[16]S. L. Chin, K. X. He, and F. Yergeau (unpublished).
[17]S. N. Dixit and P. Lambropoulos, Phys. Rev. A 27, 861 (1983).
[18]G. Leuchs and H. Walther (unpublished).